

Loss-of-function variants in *TBC1D32* underlie syndromic hypopituitarism

Johanna Hietamäki, BM^{1*}, Louise C. Gregory, PhD^{2*}, Sandy Ayoub, BSc³, Anna-Pauliina Iivonen, MSc⁴, Kirsi Vaaralahti, PhD⁴, Xiaonan Liu, MSc⁵, Nina Brandstack, MD, PhD⁶, Andrew J. Buckton, PhD⁷, Tiina Laine, MD, PhD¹, Johanna Käsäkoski, PhD⁴, Matti Hero MD, PhD¹, Päivi J. Miettinen MD, PhD¹, Markku Varjosalo MSc, PhD⁵, Emma Wakeling, PhD³, Mehul T. Dattani MBBS, MD, Prof.^{2,8*}, Taneli Raivio, MD, PhD, Prof.^{1,4*}

¹Helsinki University Hospital, New Children's Hospital, Pediatric Research Center, Helsinki 00029, Helsinki, Finland; ²Genetics and Genomic Medicine Programme, UCL Great Ormond Street Institute of Child Health, London WC1N 1EH, United Kingdom; ³North West Thames Regional Genetic Service, London North West University Healthcare NHS Trust, Harrow, UK; ⁴Department of Physiology, Medicum Unit, and Translational Stem Cell Biology and Metabolism Research Program, Faculty of Medicine, University of Helsinki, Helsinki 00014, Finland; ⁵Institute of Biotechnology & HiLIFE, University of Helsinki, 00014 Helsinki, Finland; ⁶Department of Radiology, Helsinki University Hospital and University of Helsinki, HUS 00029, Helsinki, Finland; ⁷London North Genomic Laboratory Hub, Great Ormond Street Hospital NHS Trust, London, UK; ⁸Department of Paediatric Endocrinology, Great Ormond Street Hospital for Children, London WC1N 3JH; Genetics and Genomic Medicine Programme, UCL GOS Institute of Child Health

*Equal contribution

Corresponding author: Prof. Mehul T. Dattani MBBS, MD; e-mail m.dattani@ucl.ac.uk, telephone +44 207 905 2657.

Reprint requests: Prof. Taneli Raivio, MD, PhD; e-mail taneli.raivio@helsinki.fi

© Endocrine Society 2020. jc.2019-40706. See endocrine.org/publications for Accepted Manuscript disclaimer and additional information.

This is an Open Access article distributed under the terms of the Creative Commons Attribution License (<http://creativecommons.org/licenses/by/4.0/>), which permits unrestricted reuse, distribution, and reproduction in any medium, provided the original work is properly cited.

Short title: TBC1D32 variants in hypopituitarism

Keywords: TBC1D32, hypopituitarism, Sonic hedgehog signaling, ciliopathy, retinal dystrophy

This work was supported by Academy of Finland, Foundation for Pediatric Research, and Sigrid Juselius Foundation for T.R. The research was also made possible through access to patients being recruited to the 100,000 Genomes Project. The 100,000 Genomes Project uses data provided by patients and collected by the UK National Health Service (NHS) as part of their care and support. The 100,000 Genomes Project is managed by Genomics England Limited (a wholly owned company of the Department of Health) and is funded by the NIHR and NHS England. The Wellcome Trust, Cancer Research UK and the Medical Research Council have also funded research infrastructure. MTD receives funding from the Great Ormond Street Hospital Children's Charity and the Medical Research Foundation, UK. Research at GOSH benefits from funding received from the NIHR Biomedical Research Centre.

Disclosure summary: The authors have nothing to disclose

ABSTRACT

CONTEXT Congenital pituitary hormone deficiencies with syndromic phenotypes, and/or familial occurrence suggest genetic hypopituitarism; however, in many such patients the underlying molecular basis of the disease remains unknown.

OBJECTIVE To describe patients with syndromic hypopituitarism due to biallelic loss-of-function variants in *TBC1D32*, a gene implicated in Sonic hedgehog (Shh) signaling.

SETTING Referral center

PATIENTS A Finnish family of two siblings with panhypopituitarism, absent anterior pituitary, and mild craniofacial dysmorphism, and a Pakistani family with a proband with growth hormone deficiency, anterior pituitary hypoplasia, and developmental delay.

INTERVENTIONS The patients were investigated by whole genome sequencing. Expression profiling of *TBC1D32* in human fetal brain was performed through *in situ* hybridization. Stable and dynamic protein-protein interaction partners of TBC1D32 were investigated in HEK cells followed by mass spectrometry analyses.

MAIN OUTCOME MEASURES Genetic and phenotypic features of patients with biallelic loss-of-function mutations in *TBC1D32*.

RESULTS The Finnish patients harboured compound heterozygous loss-of-function variants (c.1165_1166dup p.(Gln390Phefs*32), and c.2151del p.(Lys717Asnfs*29)) in *TBC1D32*; the Pakistani proband carried a known pathogenic homozygous *TBC1D32* splice-site variant c.1372+1G>A p.(Arg411_Gly458del), as did a fetus with cleft lip and partial intestinal malrotation from a terminated pregnancy within the same pedigree. *TBC1D32* was expressed in the developing hypothalamus, Rathke's pouch and areas of the hindbrain. TBC1D32 interacted with proteins implicated in cilium assembly, Shh signaling, and brain development.

CONCLUSIONS Biallelic *TBC1D32* variants underlie syndromic hypopituitarism, and the underlying mechanism may be via disrupted Shh signaling.

Accepted Manuscript

INTRODUCTION

Pituitary hormone deficiencies in combination with extra-pituitary manifestations suggest a role for genes involved in the early patterning of the pituitary, such as *HESX1*, *PITX2*, *OTX2*, *SOX2*, *SOX3*, *LHX3*, *LHX4*, *GLI2*, and *FGF8*, that form a complex cascade culminating in the formation of midline anterior brain and craniofacial structures (1-6). However, in the majority of cases, the underlying molecular basis remains unknown. The Sonic hedgehog (Shh) signaling pathway is essential for central nervous system (CNS), early pituitary and ventral forebrain development in mice. Pathogenic variants in components of the SHH pathway have been described in patients with holoprosencephaly, isolated congenital hypopituitarism, and cranial/midline facial abnormalities (7). Variably penetrant variants in *GLI2*, a zinc-finger transcription factor that mediates SHH transduction, have been described in patients with variable holoprosencephaly phenotypes, including microcephaly, bilateral cleft lip/palate, postaxial polydactyly, optic nerve hypoplasia, and an absent/hypoplastic pituitary with isolated or multiple anterior pituitary hormone deficiencies (8). *GLI2* variants are not infrequently associated with combined pituitary hormone deficiency in isolation, without midline defects or other features of holoprosencephaly (9).

Extra-pituitary phenotypic features in patients with complex forms of hypopituitarism may be suggestive of certain genotypes, and are important in guiding molecular studies (1). Herein, we utilized whole genome sequencing (WGS) to identify the molecular basis of hypopituitarism in three patients who presented with pituitary hormone deficiencies and craniofacial phenotypes, together with variable limb, intellectual and retinal phenotypes. Our results show that the patients carried biallelic loss-of-function variants in *TBC1D32*, a gene implicated in ciliary function and sonic hedgehog signaling (10,11). We subsequently investigated the expression of *TBC1D32* in the developing human brain, and

examined its protein-protein interaction partners to gain insight into the putative disease mechanism by which variants in this gene cause such a complex phenotype.

MATERIALS AND METHODS

Patients and clinical data

We investigated a Finnish family (Pedigree I, **Fig. 1A**) including two affected siblings with an absent anterior pituitary, ectopic posterior pituitary, mild craniofacial dysmorphism, and progressive retinal dystrophy, and a consanguineous Pakistani family (Pedigree II, **Fig. 1A**) with a proband who presented with developmental delay and features suggestive of oral-facial-digital syndrome (OFDS) associated with growth hormone (GH) deficiency. Detailed pedigrees are documented in the Results section.

Genetics

Genomic DNA was extracted from the subject's peripheral blood leukocytes. WGS of the Finnish family was performed in the Beijing Genomic Institute (BGI, Shenzhen, China) with Illumina HiSeq X Ten technology. On the basis of pedigree I, a recessive mode of inheritance was assumed to be most likely. Therefore, filtering analysis of the WGS data searched for either homozygous or compound heterozygous variants that were present in both patients, where the parents carried only one in a heterozygous state. We only considered non-synonymous or splice site variants that were novel or had frequencies of less than 0.5%. WGS of the Pakistani family was carried out via the 100,000 Genomes Project: Protocol v3, Genomics England. (12) A number of standardized panels from Genomics England PanelApp were subsequently applied to the data from Pedigree II (13), including a panel for rare,

multisystem ciliopathy disorders (v1.28). Targeted sequence analysis by bidirectional Sanger sequencing was used to confirm the presence and the mono-/biallelicity of the likely pathogenic variants.

Reverse transcriptase PCR analysis

A 310-bp fragment of the *TBC1D32* transcript was amplified from the human pituitary gland and hypothalamic cDNA, respectively, (QUICK-Clone pituitary cDNA, Takarabio, 1.5µl / reaction, Hypothalamus Marathon®-Ready cDNA, Takarabio, 1.5µl / reaction) using cDNA-specific primers. *GAPDH* served as a reference gene. The PCR products were visualized on a 1% agarose gel.

Human embryonic expression analysis: in situ hybridisation

A purified pT7T3D-PacI vector containing a portion of the human wild-type *TBC1D32* cDNA (IMAGE ID: 505804) (Source Bioscience) was used to make both the antisense and control sense digoxigenin-labelled *TBC1D32* RNA probes. Human embryonic tissue sections were selected at Carnegie stage (CS) 19, 20 and 23 (equivalent to gestational age 6, 7 and 8 weeks into development) respectively, obtained from the Human Developmental Biology Resource (HDBR). Due to limited access to human embryonic tissue, we were restricted to these three stages during embryogenesis. The *in situ* hybridisation protocol was performed as previously described (14), to generate a human embryonic expression brain profile incorporating the hypothalamo-pituitary region. More detailed information on restriction enzymes and RNA sequences are available upon request.

Cell culture, affinity purification and mass spectrometry

The *TBC1D32* PCR-product with flanking at B sites was used for BP reaction to generate the gateway compatible entry clone. LR recombination was performed between the entry clones and the destination vector to generate the MAC-tag tagged *TBC1D32* expression vector (15). Culture of Flp-In T-REx 293 (ThermoFischer Scientific) cell lines, transfection, and stable cell line selection were performed as previously described (16,17). Affinity purification (AP) and BioID experiments together with mass spectrometry (MS) analysis were performed as previously described (18).

Ethics

The study was approved by the Ethics Committee of the Hospital District of Helsinki and Uusimaa (Committee for women, children and psychiatry, approval HUS/3325/2017). Full informed consent was obtained from the UK family to participate in the 100,000 Genomes Project. The guardians of the patients gave their written informed consents to participate in the phenotyping and genetic studies. Written consent for publication of photographs was also obtained from the parents of the proband in the Pakistani family and from the parents of the Finnish family.

RESULTS

Pedigree I: A Finnish family with healthy parents, two affected children and one unaffected child, is shown in **Fig. 1A**. Patient I.3 (**Fig. 1A**) was born at 42+1 weeks gestation following an uncomplicated pregnancy. Labor was induced due to postmaturity, and proceeded to an emergency caesarean section due to changes in the CTG-scan. The patient had birth asphyxia

with Apgar scores of 1/4/5 at 0/5/15 minutes of age, respectively. He was hydropic, hypotonic, and had recurrent hypoglycemia, jaundice, and transient diabetes insipidus. Although the post-term ultrasound scan at GW 41+1 had shown short fetal femoral bones, his birth length (50.2 cm, -1.0 SDS), weight (3.51 kg, -0.8 SDS), and head circumference (38.0 cm, +1.6 SDS), were within normal limits. He was treated with intermittent nasal-CPAP, short intubation and phototherapy, and had a patent ductus arteriosus (PDA) which closed spontaneously, with no other structural cardiac anomalies. He had micropenis and bilateral cryptorchidism (corrected surgically before 2 years of age). During the first weeks of life, he was diagnosed with GH, ACTH, TSH and gonadotropin deficiencies (**Table 1**). Treatment with L-thyroxin, hydrocortisone and GH was commenced immediately. Brain MRI revealed that the sella turcica and the hypophysis were not identifiable, and an ectopic or undescended neurohypophysis was present near the tuber cinereum (**Fig. 1B**). The optic chiasm was somewhat narrow although the optic nerves were normal. In addition to the endocrine abnormalities, he had communicating hydrocephalus, developmental delay, and slight bilateral astigmatism. He was partially dependent on nasogastric tube feeding up to five months of age, and had severe secretory otitis media with insertion of grommets at the age of one year. At three years of age, he died unexpectedly following infection, in spite of adequate hydrocortisone substitution.

Patient I.5 (**Fig. 1A**), the sister of I.3, was born by vaginal delivery at 41+6 weeks gestation following an uncomplicated pregnancy. Her birth length, weight, and head circumference were 51 cm (-0.1 SDS), 3.90 kg (+0.1 SDS) and 37 cm (+1.3 SDS), respectively. She had a prominent forehead, large anterior fontanelle, and deep set eyes with low-set ears (**Fig. 1C**). She had hypotonia, hypoglycemia, and metabolic acidosis. Endocrine investigations were initiated soon after birth due to her phenotype and a positive family history of hypopituitarism. She was diagnosed with GH and TSH deficiencies (**Table 1**), and

has received GH and L-thyroxin substitution treatment since the neonatal period. In addition, the patient was commenced on oral hydrocortisone due to the family history and the possibility of progressive ACTH deficiency. MRI revealed an absent sella turcica and anterior pituitary gland, and potential neurohypophyseal tissue was detected close to the tuber cinereum (**Fig. 1B**). She had insertion of grommets before one year of age. Cardiac ultrasound and 24-hour ECG were both normal at the age of 6 months. Interestingly, she has also been diagnosed with progressive retinal dystrophy, motor delay, neuromuscular scoliosis and discrepancy of her lower limb length. Her upper jaw is narrow with misaligned teeth, of which three have by now been extracted. Due to marked feeding difficulties, she underwent speech therapy until 6 years of age. At the age of 8 years, she was prepubertal, and exhibited dysmorphic craniofacial features, including a prominent forehead, wide nasal bridge, short upturned nose, hypertelorism, downward slanting palpebral fissures, posteriorly-rotated ears, low hairline, and nuchal hair (**Fig. 1C**). She had a barrel-like chest and widely spaced nipples. Hypermobility was noted in the upper limbs. Her finger pads were prominent and she had fingernail clubbing. There was slight syndactyly of the 2nd and 3rd toes, and a bilateral sandal gap. Her cognitive development is normal.

WGS data had an average sequencing depth of at least 28.83 and 99.01% coverage for each sample. Both I.3 and I.5 carried compound heterozygous variants predicted to lead to frameshifts and premature stop codons, c.1165_1166dup p.(Gln390Phefs*32) and c.2151del p.(Lys717Asnfs*29), in the *TBC1D32* (NM_152730.5) gene (**Fig. 1A**). The mother (I.1) carried the c.2151del variant, and the father (I.2) and healthy brother (I.4) carried the c.1165_1166dup variant in a heterozygous state. The c.1165_1166dup p.(Gln390Phefs*32) (rs546631812) variant is reported in the gnomAD database with a minor allele frequency of 0.001090. The c.2151del p.(Lys717Asnfs*29) variant is absent from the gnomAD, ExAC, and SISu Project databases.

Pedigree II. An independent consanguineous pedigree with a loss-of-function variant in *TBC1D32* is presented in **Fig. 1A**. The proband (II.8) is a 5-year old girl, born to second cousin Pakistani parents (II.6 and II.7). Antenatal scans showed short long bones (femur length below 3rd centile), midline cystic changes in the brain, and polyhydramnios. Her birth weight at term was 3.27 kg (9th centile; -0.4 SDS). She was noted to have distinctive facial features with a broad forehead, wide anterior fontanelle, hypertelorism, low-set ears, flat nasal bridge, anteverted nares, slight midline groove on the tongue, serrated gums (but not overt frenulae), ankyloglossia and a high, narrow palate (**Fig. 1C**). Other findings included post-axial polydactyly on her left hand, small hands and apparent rhizomelic shortening of the limbs. After failure to pass a nasogastric tube she was found to have left-sided choanal atresia. An MRI brain scan performed at birth was reported as showing partial agenesis of the corpus callosum and a very small anterior pituitary gland and optic chiasm, consistent with septo-optic dysplasia (**Fig. 1B**). There was dysplasia of the cerebellar vermis with a midline cleft, similar to MRI scan findings observed in Joubert syndrome. Her brainstem was small, with a small interhemispheric lipoma. A skeletal survey, renal ultrasound and echocardiogram were all normal. Her head circumference at 6 months was 42.5 cm (+0.1 SDS). Her growth was suboptimal with a GH concentration of 0.6 ug/L in response to hypoglycaemia with an undetectable serum IGF-1 and a low IGFBP3 (0.75 mg/L; NR 0.8-3.9). Her cortisol was normal at 464 nmol/L. She was commenced on GH treatment at 13 months of age (height SDS -5.0) with a good response. At 4.75 years, her height was 91.2cm (-3.2 SDS).

She has global developmental delay and attends a special needs school. She sat independently at 2 years. However, at 5.5 years she is still unable to mobilize independently, although she will stand with support. She does not vocalize but understands familiar words.

At 3 years of age, she had grommet insertion for bilateral glue ear and her hearing is currently normal. She has a bilateral divergent squint and severe cerebral visual impairment with reduced visual acuity but with normal retinal responses on electroretinogram. WGS showed that patient II.8 was homozygous for a variant (NM_152730.5; c.1372+1G>A) in *TBC1D32* (**Fig. 1A**). This variant was previously reported in association with OFDS type IX (19) and is predicted to cause aberrant splicing by abolishing the exon 12 splice site, resulting in exon skipping of exon 12, with a truncation of the protein, p.(Arg411_Gly458del), and was therefore considered pathogenic. In her mother's second pregnancy, the fetus (II.9) was found to have midline facial clefting and a femoral length below the 3rd centile on ultrasound scan at 20 weeks gestation. The parents opted for a termination of pregnancy. Postmortem examination showed a female fetus with midline cleft lip and partial intestinal malrotation. Targeted sequence analysis by bidirectional Sanger sequencing confirmed the presence of the homozygous variant in both the proband and fetus (**Fig. 1A**). Parental testing, also by Sanger sequencing, confirmed their carrier status. Subsequently, the mother has given birth to healthy twin boys, who have not been genetically tested.

Human embryonic and adult *TBC1D32* expression analysis

In situ hybridization studies showed that human *TBC1D32* expression during embryonic brain development is not prominent in the hypothalamus or Rathke's pouch at Carnegie stage (CS) 19 or 20 (**Fig. 2A-B**). However, at CS23, *TBC1D32* is expressed in the hypothalamus, Rathke's pouch, trigeminal ganglia and choroid plexus (**Fig. 2C,D**), with strong expression throughout the hindbrain and thalamus at this stage (**Fig. 2D**). Additionally, *TBC1D32* is expressed in both adult human pituitary and hypothalamic cDNA libraries (**Fig. 3**).

Protein-protein interaction partners of TBC1D32

We employed a MAC-tag approach (15) to comprehensively identify the interaction partners of TBC1D32 (a.k.a broad-minded, BROMI) by performing affinity purification (AP) and proximity labeling (BioID), followed by MS. Using a comparative statistical analysis (15), we identified a total of 81 high confidence interacting proteins (HCIPs) (20), and subsequently, the DAVID functional annotation clustering tool (21) and primary cilium database (22) were used to group the related proteins. The results are shown in **Fig. 4**. In brief, the 81 interactors were mapped to 13 different cellular gene ontology classes: hedgehog signaling, cilium assembly, extracellular exosome, membrane, small GTPase-mediated signal transduction, transport, cell cycle, brain development, oxidation reduction process, positive regulation of cytokinesis, transmembrane transporter activity, acquired immunodeficiency syndrome, and intracellular protein transport. The analysis disclosed 25 novel interactors of TBC1D32 that were grouped in the following six classes: transport; small GTPase mediated signal transduction; membrane; intracellular protein transport; transmembrane transporter activity; extracellular exosome (**Fig. 4**). We performed both AP and proximity labeling (BioID) coupled with MS for TBC1D32. The TBC proteins are a group of Rab-GAP (GTPase-activating protein) proteins, which are involved in plasma membrane-endosome trafficking processes (23). Another critical group of proteins interacting with TBC1D32 (13 prey proteins), belongs to acquired immune deficiency syndrome and provides a putative link between the immune system and TBC1D32 function. Notably, four interacting proteins were associated with the oxidation-reduction process, and three proteins were linked to brain development.

DISCUSSION

To date, biallelic *TBC1D32* variants have been described in one male patient with severe facial and ocular phenotypes, microcephaly, post-axial polydactyly and CNS abnormalities including the absence of the pituitary gland with subsequent panhypopituitarism (19). Herein, we describe phenotypic features of three children and one aborted fetus from two unrelated pedigrees, that are affected by biallelic loss-of-function variants in *TBC1D32*. Our results, together with those of Adly *et al.*, confirm that *TBC1D32* variants underlie a recessive disorder demarcated by severe but highly variable expression of midline defects, including congenital hypopituitarism due to abnormal hypothalamo-pituitary development.

OFDSs are clinically and genetically heterogeneous ciliopathies characterized by abnormalities of the face, oral cavity and extremities (24). To date, at least 13 OFDS subtypes and 16 associated genes have been reported (24,25). Comparison of the phenotypic features of the patients in our study and the patient with OFDS type IX reported by Adly *et al.* (19) is shown in **Table 2**. It is noteworthy that the recurring splice-site variant is associated with postaxial polydactyly, but variable ocular and oral phenotypes (**Table 2**), consistent with variable expressivity. In contrast, the Finnish siblings carrying two other loss-of-function variants in *TBC1D32* did not exhibit postaxial polydactyly, but had variable intellectual and ocular phenotypes. A unifying theme in all four patients reported to date, however, is the pituitary gland phenotype, with variable pituitary hormone deficiencies (**Table 2**). The CNS phenotype of the aborted fetus is not available; however, the fetus also carried the homozygous *TBC1D32* p.Arg411_Gly458del truncation and displayed cleft lip and intestinal malrotation, adding the latter feature to the list of associated phenotypes in biallelic *TBC1D32* loss-of-function variant carriers. Human gene expression analysis in our study identified *TBC1D32* expression in the developing hypothalamus and pituitary gland

(CS23) (**Fig. 2C**), and in pituitary and hypothalamic cDNA libraries of adults (**Fig. 3**), suggesting activation of this gene during the early stages of hypothalamo-pituitary formation during embryogenesis, which is maintained into adulthood. Furthermore, the strong *TBC1D32* expression seen in other areas of the hindbrain (**Fig. 2D**) suggests that *TBC1D32* plays a role in other regions of the brain during development, possibly reflective of the complex variable CNS problems seen in OFDS patients such as ours.

Previous proteomic analysis of cilia has confirmed that *TBC1D32* is a ciliary protein (26). Cilia can be motile or non-motile (primary cilia) and are specialized microtubule-based sensory organelles (27), which play a role in cell polarity determination and in mediating vital signaling cascades such as the SHH signaling pathway (28). Therefore, the correct development of cilia is a prerequisite for SHH signaling. Deletion of the *Tbc1d32* homolog in mice, referred to as the *Bromi* mouse, causes a severe phenotype encompassing developmental defects including a lack of the neural tube floor plate, exencephaly, signs of defective ventral neural fate specification, poorly developed eyes, and preaxial polydactyly. Electron microscopy of the neuroepithelium in these mice showed curled axonemes surrounded by dilated ciliary membranes. These studies showed that *Bromi*-mutant neurons were associated with deficient Shh signaling activation of downstream regulators *Gli2* and *Gli3*, and that *Tbc1d32* is critical for the correct localization of *Gli2* within the cilium (10). A similar phenotype to the *Bromi* mouse was also noted in morpholino-mediated knockdown studies of the gene homolog in zebrafish (10). Hence, these studies provide a clear link between ciliary morphology and the correct localization of *Gli2* in the cilia, and suggest that the hypopituitary phenotype observed in association with *TBC1D32* variants in humans is likely the result of *GLI2* mislocalization. Recently, mutation in *IFT172* has been associated with a phenotype characterized by anterior pituitary hypoplasia, an ectopic posterior pituitary, retinopathy, metaphyseal dysplasia, and renal failure (29). *IFT172* has been implicated in

ciliary function, and hence our study provides further support for the role of cilia in hypothalamo-pituitary disease.

In mammalian cells, primary cilia are essential for SHH signaling (30), and in protein-protein interaction studies, we identified ten proteins of HCIPs that are involved in the assembly of primary cilia (**Fig. 4**). Our analyses confirmed that TBC1D32 interacts with histone deacetylase 1 (HDAC1), a protein implicated in SHH signaling (31), and interacts with two additional prey proteins (FKBP8, DHCR7) that regulate SHH signaling (32-37) (**Fig. 4**). Furthermore, the loss of mouse cell cycle-related kinase (CCRK) function, a protein known to interact with TBC1D32 (10), has been shown to result in a highly similar embryonic phenotype to that of the *Bromi* null mouse, resulting in disrupted optic cup and lens formation, shortened optic stalk, reduced neural retina specification, and ectopic retinal pigment epithelium formation (10,38,39). Although our experiment using a human cell line did not find an association with CCRK, five TBC1D32-interacting proteins (C1114, UHRF1, AURKB, CENPV, SVIL) were associated with positive regulation of cytokinesis and the cell cycle (**Fig. 4**). Taken together, proteomics provided a conceivable link between TBC1D32 and the developmental defects of the pituitary gland and the eye. Although we found a connection between TBC1D32 and regulators of the immune system, its association with the recurrent ear infections seen in all the patients and the unexpected death of patient I.3 remains to be established. It is important to note, however, that patients I.5 and II.8 do not have a history of recurrent or severe infections. Immune function or ciliary function have not been examined in detail in any of the patients.

To conclude, we describe three patients and an aborted fetus with biallelic variants in *TBC1D32*, a ciliary gene implicated in SHH signaling and leading to the correct localization of Gli2, a protein that is significantly implicated in the aetiology of congenital hypopituitarism and related disorders. The available evidence to date suggests that this defect

should be suspected in patients with pituitary hormone deficiencies and craniofacial phenotypes, even in the absence of retinal dystrophy, oral phenotype, intellectual disability, or postaxial polydactyly. Finally, our results generated a developmental human brain expression profile of *TBC1D32*, confirmed the role of *TBC1D32* as an interacting partner of HDAC1, and highlighted its connections to cilia assembly, SHH signal transduction, the immune system, and the regulation of the cell cycle. The immune system and cell cycle related *TBC1D32* functions may modify the phenotype of patients with *TBC1D32* mutations, and suggest an interesting direction for future studies.

Accepted Manuscript

REFERENCES

1. Fang Q, George AS, Brinkmeier ML, Mortensen AH, Gergics P, Cheung LYM, Daly AZ, Ajmal A, Pérez Millán MI, Ozel AB, Kitzman JO, Mills RE, Li JZ, Camper SA. Genetics of combined pituitary hormone deficiency: Roadmap into the genome era. *Endocr Rev.* 2016;37(6):636-675.
2. Bancalari RE, Gregory LC, McCabe MJ, Dattani MT. Pituitary gland development: An update. In: Mullis P-E, ed. *Developmental Biology of GH Secretion, Growth and Treatment.* *Endocr Dev.* Basel: Karger; 2012;23:1-15.
3. McCabe MJ, Dattani MT. Genetic aspects of hypothalamic and pituitary gland development. In: *Handb Clin Neurol.* Netherlands: Elsevier B.V; 2014;124:3-15.
4. de Moraes DC, Vaisman M, Conceicao FL, Ortiga-Carvalho TM. Pituitary development: A complex, temporal regulated process dependent on specific transcriptional factors. *J Endocrinol.* 2012;215(2):239-245.
5. Kelberman D, Rizzoti K, Lovell-Badge R, Robinson IC, Dattani MT. Genetic regulation of pituitary gland development in human and mouse. *Endocr Rev.* 2009;30(7):790-829.
6. Castinetti F, Reynaud R, Saveanu A, Jullien N, Quentien MH, Rochette C, Barlier A, Enjalbert A, Brue T. MECHANISMS IN ENDOCRINOLOGY: An update in the genetic aetiologies of combined pituitary hormone deficiency. *Eur J Endocrinol.* 2016;174(6):R239-R247.

7. Wang Y, Martin JF, Bai CB. Direct and indirect requirements of Shh/Gli signaling in early pituitary development. *Dev Biol.* 2010;348(2):199-209.
8. Roessler E, Du YZ, Mullor JL, Casas E, Allen WP, Gillessen-Kaesbach G, Roeder ER, Ming JE, Ruiz i Altaba A, Muenke M. Loss-of-function mutations in the human GLI2 gene are associated with pituitary anomalies and holoprosencephaly-like features. *Proc Natl Acad Sci U S A.* 2003;100(23):13424-13429.
9. Gregory LC, Gaston-Massuet C, Andoniadou CL, Carreno G, Webb EA, Kelberman D, McCabe MJ, Panagiotakopoulos L, Saldanha JW, Spoudeas HA, Torpiano J, Rossi M, Raine J, Canham N, Martinez-Barbera JP, Dattani MT. The role of the sonic hedgehog signalling pathway in patients with midline defects and congenital hypopituitarism. *Clin Endocrinol (Oxf).* 2015;82(5):728-738.
10. Ko HW, Norman RX, Tran J, Fuller KP, Fukuda M, Eggenschwiler JT. Broad-minded links cell cycle-related kinase to cilia assembly and hedgehog signal transduction. *Dev Cell.* 2010;18(2):237-247.
11. Reiter JF, Leroux MR. Genes and molecular pathways underpinning ciliopathies. *Nat Rev Mol Cell Biol.* 2017;18:533-547.
12. The National Genomics Research and Healthcare Knowledgebase v3, Genomics England. 2017. doi: 10.6084/m9.figshare.4530893.v3. Accessed: 2018.

13. Genomics england PanelApp. <https://panelapp.genomicsengland.co.uk>. Accessed: 2018.
14. Gregory LC. Investigation of new candidate genes in a cohort of patients with familial congenital hypopituitarism and associated disorders. Dissertation, London: University College London. 2016.
15. Liu X, Salokas K, Tamene F, Jiu Y, Weldatsadik RG, Öhman T, Varjosalo M. An AP-MS- and BioID-compatible MAC-tag enables comprehensive mapping of protein interactions and subcellular localizations. *Nat Commun.* 2018;9:1188.
16. Varjosalo M, Sacco R, Stukalov A, van Drogen A, Planyavsky M, Hauri S, Aebersold R, Bennett KL, Colinge J, Gstaiger M, Superti-Furga G. Interlaboratory reproducibility of large-scale human protein-complex analysis by standardized AP-MS. *Nat Methods.* 2013;10:307-314.
17. Heikkinen T, Kämpjärvi K, Keskitalo S, von Nandelstadh P, Liu X, Rantanen V, Pitkänen E, Kinnunen M, Kuusanmäki H, Kontro M, Turunen M, Mäkinen N, Taipale J, Heckman C, Lehti K, Mustjoki S, Varjosalo M, Vahteristo P. Somatic MED12 nonsense mutation escapes mRNA decay and reveals a motif required for nuclear entry. *Hum Mutat.* 2017;38(3):269-274.
18. Yadav L, Tamene F, Göös H, van Drogen A, Katainen R, Aebersold R, Gstaiger M, Varjosalo M. Systematic analysis of human protein phosphatase interactions and dynamics. *Cell Syst.* 2017;4(4):430-444.e5.

19. Adly N, Alhashem A, Ammari A, Alkuraya FS. Ciliary genes *TBC1D32/C6orf170* and *SCLT1* are mutated in patients with OFD type IX. *Hum Mutat.* 2014;35(1):36-40.
20. Hietamäki J, Gregory LC, Ayoub S, Iivonen A-P, Vaaralahti K, Liu X, Brandstack N, Buckton AJ, Laine T, Käsäkoski J, Hero M, Miettinen PJ, Varjosalo M, Wakeling E, Dattani M, Raivio T. Data from: Loss-of-function variants in *TBC1D32* underlie syndromic hypopituitarism. Figshare Digital Repository 2020. Deposited 06 January 2020. DOI: 10.6084/m9.figshare.11522793.
21. Huang DW, Sherman BT, Tan Q, Collins JR, Alvord WG, Roayaei J, Stephens R, Baseler MW, Lane HC, Lempicki RA. The DAVID gene functional classification tool: A novel biological module-centric algorithm to functionally analyze large gene lists. *Genome Biol.* 2007;8:R183.
22. Mirvis M, Siemers KA, Nelson WJ, Stearns TP. Primary cilium loss in mammalian cells occurs predominantly by whole-cilium shedding. *PLoS Biol.* 2019;17(7):e3000381.
23. Barr F, Lambright DG. Rab GEFs and GAPs. *Curr Opin Cell Biol.* 2010;22(4):461-470.
24. Bruel A-L, Franco B, Duffourd Y, Thevenon J, Jegou L, Lopez E, Deleuze JF, Doummar D, Giles RH, Johnson CA, Huynen MA, Chevrier V, Burglen L, Morleo M, Desguerres I, Pierquin G, Doray B, Gilbert-Dussardier B, Reversade B, Steichen-Gersdorf E, Baumann C, Panigrahi I, Fargeot-Espaliat A, Dieux A, David A, Goldenberg A, Bongers E, Gaillard D, Argente J, Aral B, Gigot N, St-Onge J, Birnbaum D, Phadke SR, Cormier-Daire V, Eguether T, Pazour GJ, Herranz-Pérez V, Goldstein JS, Pasquier L, Loget P, Saunier S, Mégarbané A,

Rosnet O, Leroux MR, Wallingford JB, Blacque OE, Nachury MV, Attie-Bitach T, Rivière J-B, Faivre L, Thauvin-Robinet C. Fifteen years of research on oral-facial-digital syndromes: From 1 to 16 causal genes. *J Med Genet.* 2017;54:371-380.

25. Online mendelian inheritance in man, OMIM®. Johns Hopkins University, Baltimore, MD. Phenotypic series: PS311200. <https://omim.org/phenotypicSeries/PS311200>.

26. Ishikawa H, Thompson J, Yates JR 3rd, Marshall WF. Proteomic analysis of mammalian primary cilia. *Curr Biol.* 2012;22(5):414-419.

27. Eggenschwiler JT, Anderson KV. Cilia and developmental signaling. *Annu Rev Cell Dev Biol.* 2007;23:345-373.

28. Nozawa YI, Lin C, Chuang P-T. Hedgehog signaling from the primary cilium to the nucleus: An emerging picture of ciliary localization, trafficking and transduction. *Curr Opin Genet Dev.* 2013;23(4):429-437.

29. Lucas-Herald AK, Kinning E, Iida A, Wang Z, Miyake N, Ikegawa S, McNeilly J, Ahmed SF. A case of functional growth hormone deficiency and early growth retardation in a child with IFT172 mutations. *J Clin Endocrinol Metab.* 2015;100(4):1221-1224.

30. Yabut OR, Pleasure SJ. Sonic hedgehog signaling rises to the surface: Emerging roles in neocortical development. *Brain Plast.* 2018;3(2):119-128.

31. Boldt K, van Reeuwijk J, Lu Q, Koutroumpas K, Nguyen T-MT, Texier Y, van Beersum SEC, Horn N, Willer JR, Mans DA, Dougherty G, Lamers IJC, Coene KLM, Arts HH, Betts MJ, Beyer T, Bolat E, Gloeckner CJ, Haidari K, Hetterschijt L, Iaconis D, Jenkins D, Klose F, Knapp B, Latour B, Letteboer SJF, Marcelis CL, Mitic D, Morleo M, Oud MM, Riemersma M, Rix S, Terhal PA, Toedt G, van Dam TJP, de Vrieze E, Wissinger J, Wu KM, Apic G, Beales PL, Blacque OE, Gibson TJ, Huynen MA, Katsanis N, Kremer H, Omran H, van Wijk E, Wolfrum U, Kepes F, Davis EE, Franco B, Giles RH, Ueffing M, Russell RB, Roepman R, UK10K Rare Diseases Group. An organelle-specific protein landscape identifies novel diseases and molecular mechanisms. *Nat Commun.* 2016;7:11491.
32. Bulgakov OV, Eggenschwiler JT, Hong D-H, Anderson KV, Li T. FKBP8 is a negative regulator of mouse sonic hedgehog signaling in neural tissues. *Development.* 2004;131:2149-2159.
33. Cho A, Ko HW, Eggenschwiler JT. FKBP8 cell-autonomously controls neural tube patterning through a Gli2- and Kif3a-dependent mechanism. *Dev Biol.* 2008;321(1):27-39.
34. Saita S, Shirane M, Ishitani T, Shimizu N, Nakayama KI. Role of the ANKMY2-FKBP38 axis in regulation of the Sonic hedgehog (Shh) signaling pathway. *J Biol Chem.* 2014;289:25639-25654.
35. Blassberg R, Macrae JI, Briscoe J, Jacob J. Reduced cholesterol levels impair smoothed activation in Smith-Lemli-Opitz syndrome. *Hum Mol Genet.* 2016;25(4):693-705.

36. Koide T, Hayata T, Cho KWY. Negative regulation of Hedgehog signaling by the cholesterologenic enzyme 7-dehydrocholesterol reductase. *Development*. 2006;133:2395-2405.
37. Xiao WL, Zhang D-Z, Xu H, Zhuang C-Z. Dhcr7 regulates palatal shelf fusion through regulation of Shh and Bmp2 expression. *Biomed Res Int*. 2016;2016:7532714.
38. Snouffer A, Brown D, Lee H, Walsh J, Lupu F, Norman R, Lechtreck K, Ko HW, Eggenschwiler J. Cell cycle-related kinase (CCRK) regulates ciliogenesis and hedgehog signaling in mice. *PLoS Genet*. 2017;13(8):e1006912.
39. Lupu FI, Burnett JB, Eggenschwiler JT. Cell cycle-related kinase regulates mammalian eye development through positive and negative regulation of the Hedgehog pathway. *Dev Biol*. 2018;434(1):24-35.

Accepted Manuscript

Abbreviations

ACTH	Adrenocorticotropin
AP	Affinity purification
CCRK	Cell-cycle related kinase
cDNA	Complementary DNA
CNS	Central nervous system
CS	Carnegie stage
CTG-scan	Cardiotocography
ECG	Electrocardiogram
GAP	GTPase-activating protein
GH	Growth hormone
GW	Gestational week
HCIP	High confidence interacting protein
HDAC1	Histone deacetylase I
IGF-1	Insulin-like growth factor 1
IGFBP3	Insulin-like growth factor-binding protein 3
OFDS	Oral-facial-digital syndrome
MRI	Magnetic resonance imaging
MS	Mass spectrometry
PCR	Polymerase chain reaction
PDA	Patent ductus arteriosus
SDS	Standard deviation score
Shh/SHH	Sonic hedgehog
TSH	Thyroid-stimulating hormone

Table 1. Biochemical testing of pituitary hormone secretion in patients I.3 and I.5**Table 2. Summary of clinical features in patients with biallelic mutations in *TBC1D32***

Figure 1A The pedigrees of our patients with hypopituitarism and biallelic *TBC1D32* variants. I: the Finnish pedigree; II: the Pakistani pedigree. Patients I.3 and I.5 carried compound heterozygous and patients II.8 and II.9 homozygous variants in *TBC1D32*. The parents were heterozygous carriers of the respective variants.

Figure 1B i) and ii) The MRIs of the two Finnish patients. *Upper row*, Patient I.3. Sagittal (a) and coronal (b) T1 images without contrast enhancement. The sella turcica and the pituitary gland are not identifiable. Neurohypophyseal bright tissue is seen near the tuber cinereum (arrow). *Lower row*, Patient I.5. Sagittal (a) and axial (b) T1 images without contrast enhancement. The sella turcica and the pituitary gland are absent. Potentially neurohypophyseal bright tissue is seen near the tuber cinereum (arrow); iii) Patient II.8. *Upper row*, Sagittal (a) T1 image showing partial agenesis of corpus callosum (CC), small interhemispheric lipoma (L), small anterior pituitary (AP) and small ectopic posterior pituitary (PP). *Lower row*, Coronal image showing dysplasia of the cerebellar vermis (arrow) with an abnormal left cerebellum. The “molar tooth” sign of Joubert syndrome is also shown (filled arrow).

Figure 1C Clinical photos of the patients. **i:** Patient I.3 at 2.4 years of age. Note the prominent forehead and the low-set, posteriorly rotated ears; **ii:** Patient I.5 presented with

prominent forehead, large anterior fontanelle, and low-set ears in infancy; **iii** Patient I.5 at 10.5 years of age; **iv**: Patient II.8 in infancy showing a prominent forehead with hypertelorism, low-set ears, flat nasal bridge and anteverted nares; **v**: Patient II.8 at 5.5 years of age.

Figure 2

Human expression of *TBC1D32* mRNA transcripts in transverse brain sections at different developmental stages during embryogenesis. (A) There is no clear expression in the hypothalamus, Rathke's pouch or elsewhere in the brain when comparing results using the antisense probe and the sense probe at Carnegie stage (CS) 19. (B) At CS20 there may be some partial expression in the hypothalamus using the antisense probe, however staining is very similar to the Rathke's pouch and the hypothalamus when using the control sense probe, where some background staining is noted. (C) At CS23, there is partial expression in the trigeminal ganglia, in Rathke's pouch, and along the hypothalamus when comparing the antisense and control sense probes. (D) There is strong expression in the hindbrain, in particular the thalamus, with some expression also seen in the choroid plexus. RP, Rathke's pouch; Hyp, hypothalamus; Tri, trigeminal ganglia; CP, choroid plexus; T, thalamus.

Figure 3

Reverse transcriptase PCR analysis of *TBC1D32* expression. A 310-bp fragment of transcript encoding *TBC1D32* was amplified from human pituitary gland cDNA and from hypothalamic cDNA (QUICK-Clone pituitary cDNA, Takarabio, 1.5µl / reaction, Hypothalamus Marathon®-Ready cDNA, Takarabio, 1.5ul / reaction). Human *GAPDH* was used as a reference gene. The PCR products were visualized on a 1.0% agarose gel. p, pituitary gland; ht, hypothalamus; c, negative control without DNA template).

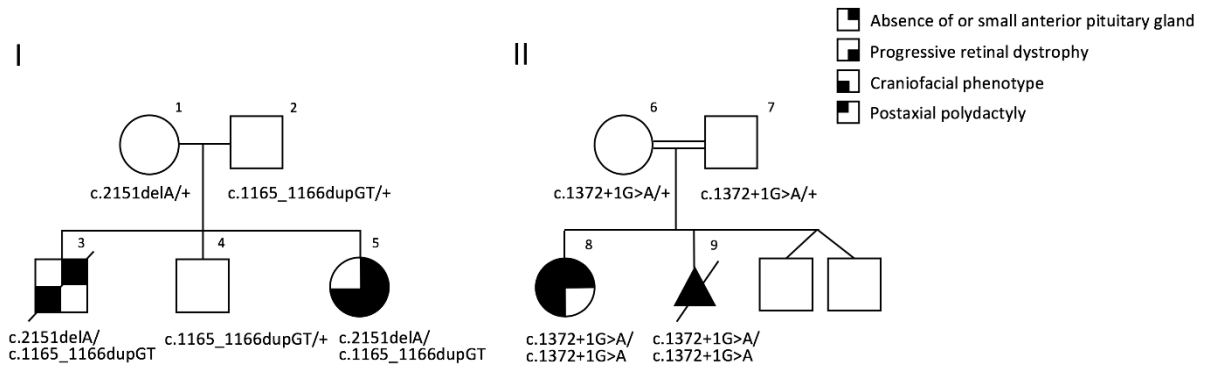
Figure 4

The functional grouping of the high confidence interacting proteins of TBC1D32.

Interactome analysis reveals known and novel interactions for TBC1D32. AP-MS and BioID analysis of TBC1D32 identified 81 high-confidence protein-protein interactions (yellow lines represent interaction detected by AP-MS approach; red lines represent interactions detected by BioID approach; overlap of the two purification methods is shown with grey line; known interaction is shown with a dashed line). The interacting proteins are grouped based on their molecular functions/complexes.

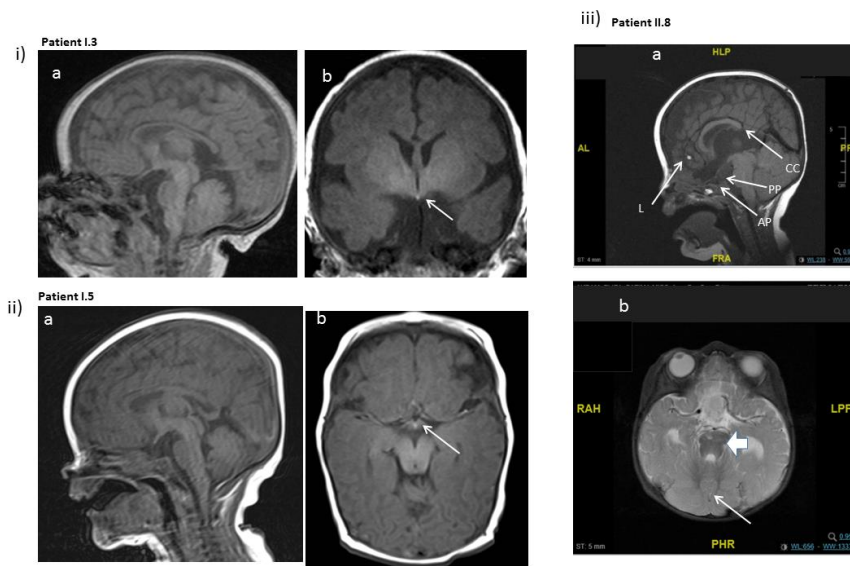
Accepted Manuscript

Figure 1A



Accepted Manuscript

Figure 1B



Accepted Manuscript

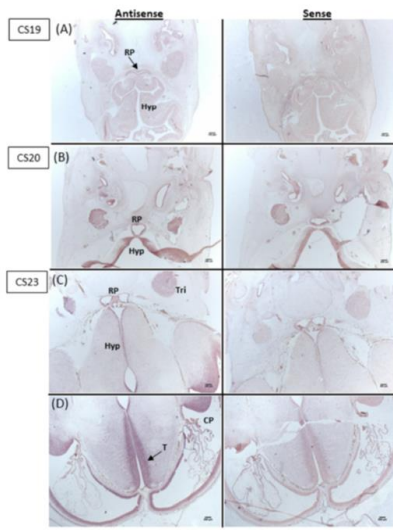


Figure 1C



Accepted

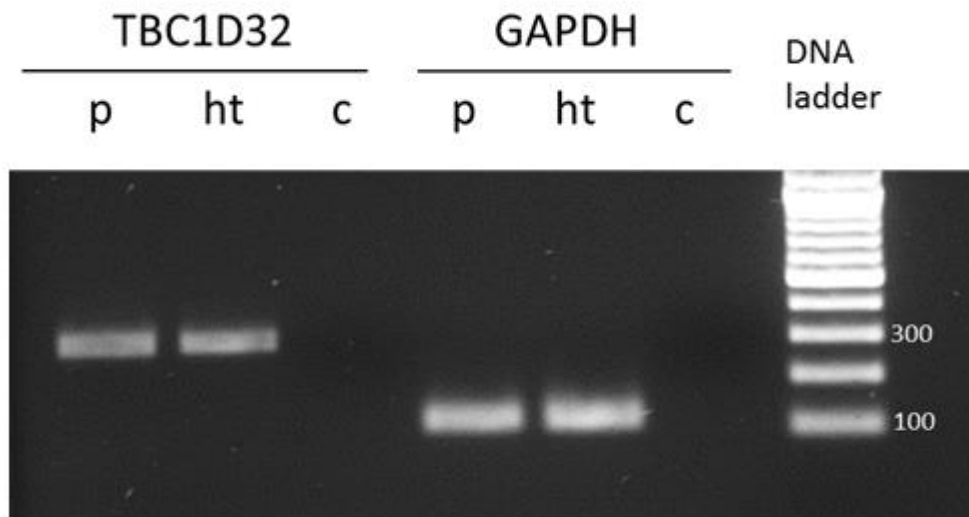
Figure 2



Accepted Manuscript

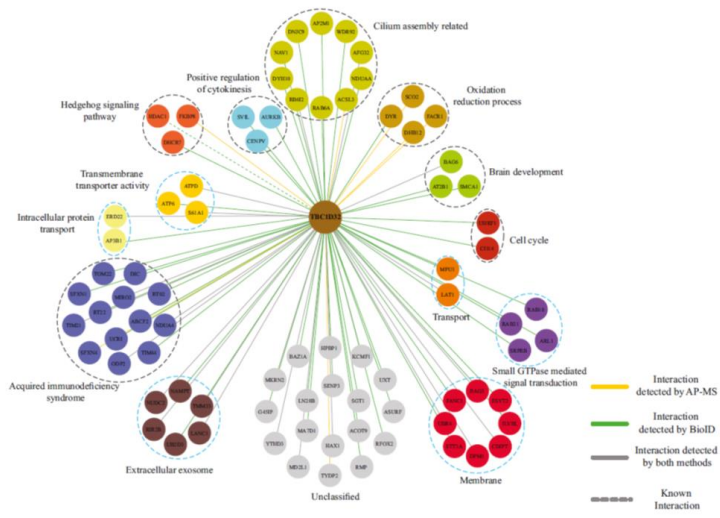
101

Figure 3



Accepted 14

Figure 4



Accepted Manuscript

Table 1. Biochemical testing of the pituitary hormone secretion in patients I.3 and I.5

	<u>Patient I.3</u>		<u>Patient I.5</u>	
	Age (days)	Test result [NR]	Age (days)	Test result [NR]
Growth hormone				
Serum IGF1 (nmol/L)	8	7 [na]	20	<3 [7-43]
Fasting serum GH during hypoglycemia (ug/L)	8	<0.03	6	0.20
Maximum arginine-stimulated serum GH (ug/L)		na	26	0.23
ACTH				
Plasma ACTH (ng/L)	14	<5 ^a [10-50]	11	15 ^a [<46]
Serum cortisol (nmol/L)	1	<20 [150-650]	11	121 ^a [30-632]
Maximum synacthen-stimulated plasma cortisol (ACTH neo test) (nmol/L)	1	<20	11	638 ^a
TSH				
Serum free T4 (pmol/L)	4	5.3 [9-19]	20	9.9 [8-25]
Serum TSH (mU/L)	4	0.002 [0.6-10]	20	2.65 [0.6-10]
Serum TSH during TRH provocation test (at 0/20/60 min) (mU/L)		na	26	2.58/4.63/4.73
Gonadotropins				
Serum inhibin B (ng/L)	2	175		na
Serum FSH (IU/L)	18	<0.10		na
Maximum serum FSH during GnRH provocation test (IU/L)	18	0.2		na
Serum LH (IU/L)	18	<0.10		na
Maximum serum LH during GnRH provocation test (IU/L)	18	<0.10		na

NR, normal range; na, not available; ^ameasured during exogenous cortisone treatment

Table 2. Summary of clinical features in patients with biallelic mutations in *TBC1D32*

	Subject I.3	Subject I.5	Subject II.8	Subject II.9	Adly <i>et al.</i> 2014 (19)
Age	3 years*	10 years	5 years	20 weeks gestation	6 months*
Sex	Male	Female	Female	Female	Male
Oral anomalies					
Bifid tongue/ midline tongue groove	-	-	+	-	-
Highly arched/cleft palate	-	-	+	-	+
Abnormal dentition	-	+	-	NA	-
Facial anomalies					
Hypertelorism	+	+	+	-	+
Midline cleft lip	-	-	-	+	+
Upturned nose	+	+	+	NA	NA
Choanal stenosis/atresia	-	-	+	NA	+
Limb anomalies					
Polydactyly	-	-	+	-	+
Syndactyly	-	+	-	-	-
Sandal gap deformity	-	+	-	-	NA
Lower limb length difference	NA	+	-	NA	NA
CNS anomalies					
Cerebellar vermis hypoplasia	-	-	+	NA	+
Hypothalamic hamartoma	-	-	-	NA	-
Agenesis of the corpus callosum	-	-	+	NA	+
Pituitary abnormalities	no anterior pituitary (ACTH, TSH, GH, and FSH/LH	no anterior pituitary (GH, TSH deficiencies),	anterior pituitary hypoplasia (GH deficiency)	NA	no pituitary gland

	deficiencies), ectopic posterior pituitary	ectopic posterior pituitary			
Basal ganglia abnormalities	-	-	+	NA	-
Brainstem abnormalities	-	-	+	NA	-
Communicating hydrocephalus	+	-	-	NA	-
Eye involvement					
Microphthalmia	-	-	-	NA	+
Retinal dystrophy	NA	progressive	-	NA	-
Coloboma	-	-	-	NA	+
Visual acuity	NA	reduced	reduced	NA	NA
Other					
Microcephaly	-	-	-	-	+
Developmental delay	global	motoric	global	NA	NA
Epileptic seizures	-	-	-	NA	+
Congenital heart disease	-	-	-	-	+
Abnormal genitalia	+	-	-	-	+
Intestinal malrotation	-	-	-	+	-
Neuromuscular scoliosis	NA	+	-	NA	NA
Chronic secretory otitis media	+	+	+	NA	NA

*age at death; +, present; -, not present; NA, not available